



**HAL**  
open science

## The open-air Paleolithic site of Mirak, northern edge of the Iranian Central Desert (Semnan, Iran): Evidence of repeated human occupations during the late Pleistocene

Hamed Vahdati Nasab, Gilles Berillon, Guillaume Jamet, Milad Hashemi, Mozghan Jayez, Somaye Khaksar, Zohreh Anvari, Guillaume Guérin, Maryam Heydari, Mohammad Akhavan Kharazian, et al.

### ► To cite this version:

Hamed Vahdati Nasab, Gilles Berillon, Guillaume Jamet, Milad Hashemi, Mozghan Jayez, et al.. The open-air Paleolithic site of Mirak, northern edge of the Iranian Central Desert (Semnan, Iran): Evidence of repeated human occupations during the late Pleistocene. *Comptes Rendus. Palevol*, 2019, 18 (4), pp.465-478. 10.1016/j.crpv.2019.02.005 . mnhn-02283751v1

**HAL Id: mnhn-02283751**

**<https://mnhn.hal.science/mnhn-02283751v1>**

Submitted on 3 Dec 2020 (v1), last revised 5 Jan 2024 (v3)

**HAL** is a multi-disciplinary open access archive for the deposit and dissemination of scientific research documents, whether they are published or not. The documents may come from teaching and research institutions in France or abroad, or from public or private research centers.

L'archive ouverte pluridisciplinaire **HAL**, est destinée au dépôt et à la diffusion de documents scientifiques de niveau recherche, publiés ou non, émanant des établissements d'enseignement et de recherche français ou étrangers, des laboratoires publics ou privés.

1 TITLE: The Open-Air Paleolithic Site of Mirak, Northern Edge of the Iranian Central Desert (Semnan,  
2 IRAN): Evidence of repeated human occupations during the late Pleistocene

3 AUTHORS NAMES AND AFFILIATIONS:

4 Hamed Vahdati Nasab<sup>1,\*</sup>, Gilles Berillon<sup>2,\*</sup>, Guillaume Jamet<sup>3</sup>, Milad Hashemi<sup>1</sup>, Mozghan Jayez<sup>4</sup>, Somaye  
5 Khaksar<sup>5</sup>, Zohreh Anvari<sup>6</sup>, Guillaume Guérin<sup>7</sup>, Maryam Heydari<sup>7</sup>, Mohammad Akhavan Kharazian<sup>1-2</sup>,  
6 Simon Puaud<sup>2</sup>, Stéphanie Bonilauri<sup>2</sup>, Valéry Zeitoun<sup>8</sup>, Noémie Sévêque<sup>9</sup>, Javad Darvishi Khatooni<sup>10</sup>, and  
7 Asghar Asgari Khaneghah<sup>11</sup>

8 1. Department of Archaeology, Tarbiat Modares University, Tehran, IRAN

9 2. UMR7194 MNHN-CNRS / Département Homme et Environnement, Musée de l'Homme - Palais de  
10 Chaillot, Paris, FRANCE

11 3. GéoArchÉon / UMR CNRS 8591 - Laboratoire de Géographie Physique, Meudon, FRANCE

12 4. Research Institute of Cultural Heritage and Tourism (RICHT), Iranian Center for Archaeological  
13 Research (ICAR), Tehran, IRAN

14 5. Department of Anthropology, University of Minnesota, USA

15 6. Faculty of Social Sciences, University of Tehran, Tehran, IRAN

16 7. IRAMAT-CRP2A, Université Bordeaux Montaigne, Maison de l'Archéologie, Pessac, FRANCE

17 8. UMR 7207-CR2P- Cnrs-Mnhn-Université Paris 6, Sorbonne universités, Université Pierre et Marie  
18 Curie, Paris, France

19 9. Laboratoire Géosystèmes, UMR 8157 CNRS, Université Lille 1, Villeneuve d'Ascq

20 10. Geological Survey of Iran, Tehran, IRAN

21 11. Institute of Research and Social Studies, Faculty of Social Sciences, University of Tehran, Tehran,  
22 IRAN

23 \* Hamed Vahdati Nasab and Gilles Berillon are both first authors

24

25 CORRESPONDING AUTHOR

26 Hamed Vahdati Nasab, [vahdati@modares.ac.ir](mailto:vahdati@modares.ac.ir)

27

28

29 ABSTRACT/RESUME

30 The northern edge of the Iranian Central Desert has provided valuable evidence for terminal Pleistocene  
31 human settlements. Mirak constitutes one of the largest open-air lithic scatters in the region, consisting  
32 of eight natural mounds. Fieldwork was initiated in 2015 by the joint Iranian-French program at Mirak 8.  
33 Preliminary results have demonstrated at least 3 successive phases of human occupation during the MIS3:  
34 an upper layer with clear Upper Paleolithic affinities and a maximum age of 28ky, a lower layer with clear  
35 Middle Paleolithic affinities that dates around 47ky, and an intermediate layer with mixed characteristics  
36 that can be seen as an intermediate Paleolithic phase which dates between  $28\pm 2$  and  $38\pm 2$  ky. At the time  
37 that Upper Paleolithic cultures originated in the Zagros Mountains, cultures with clear Middle Paleolithic  
38 affinities persisted nearby along the northern edge of the Iranian Central Plateau.

39

40 Le nord du Désert Central Iranien fournit des preuves de présence humaine à la fin du Pléistocène.  
41 Mirak constitue l'une des plus grandes localités paléolithiques de plein air de la région, avec huit  
42 monticules naturels. En 2015, le programme conjoint franco-iraniens a initié la fouille et l'étude  
43 pluridisciplinaire des dépôts et du matériel archéologique de Mirak 8. Les premiers résultats de trois  
44 saisons de fouilles, indiquent la présence d'au moins 3 phases successives d'occupation humaine  
45 pendant le MIS3 : un niveau supérieur d'affinités Paléolithique supérieur, avec un âge maximum de  
46 28ka, un niveau inférieur d'affinités Paléolithique moyen, autour de 47ka, et un niveau intermédiaire  
47 avec des caractéristiques mixtes vu comme un Paléolithique intermédiaire, daté entre  $28\pm 2$  et  $38\pm 2$ ka. A  
48 l'époque où les cultures du Paléolithique supérieur se sont différenciées dans le Zagros, des cultures  
49 avec des affinités Paléolithique moyen évidentes ont persisté juste à l'Est du Zagros sur le pourtour nord  
50 du Plateau central iranien.

51

52 **KEYWORDS/MOTS CLÉ**

53 Iranian Central Desert, Middle and Upper Paleolithic, Mirak, Late Pleistocene, Semnan

54 Desert Central Iranien, Paléolithique supérieur et moyen, Mirak, Pléistocène supérieur, Semnan

55

## 56 1. INTRODUCTION

57 The wide area extending from the Zagros-Caucasus to Central Asia is historically acknowledged as a key  
58 region for understanding prehistoric human settlements, from the first human dispersal into Eurasia  
59 during the Early Pleistocene to the Upper Pleistocene (Zeitoun, 2016), including the transition from Middle  
60 Paleolithic to Upper Paleolithic cultures (e.g., Coon, 1951; Becerra-Valdivia et al. 2017; Heydari-Guran and  
61 Ghasidian 2017; McBurney, 1964; Otte et al. 2009, 2011; Smith, 1986). However, despite the discoveries  
62 of numerous Paleolithic sites in this region and broad interest in the transition from Upper to Middle  
63 Paleolithic, to date, few archaeological assemblages have been obtained using accurate geological and  
64 chronological frameworks. These are mainly concentrated on the mountainous areas, especially the  
65 Zagros (Figure 1) and dated to the MIS3 (see Becerra-Valdivia et al., 2017 for the current chronological  
66 framework). Some of them include: Shanidar (Solecki, 1955), Warwasi (Braidwood and Howe, 1961;  
67 Tsanova, 2013), Yafteh (Hole and Flannery, 1967; Otte et al., 2011), Gar Arjeneh (Hole and Flannery, 1967;  
68 Otte and Biglari, 2004), Ghar-e Khar (Shidrang et al., 2016; Young and Smith, 1966), Guilvaran and Kaldar  
69 (Bazgir et al., 2014, 2017; Roustaei et al. 2004), Ghār-e Boof (Ghasidian et al., 2017 ; Heydari et al., 2004).  
70 Other sites have been discovered in the Zagros and along its eastern fringes during the last decade. Most  
71 of these sites lack an adequate chronological framework, such as Mar-Tarik and Qaleh Bozi (Biglari, 2000,  
72 Biglari et al. 2009; Jaubert et al., 2008, 2009) as well as Zavyeh, Qaleh Gusheh and Holabad (Heydari-  
73 Guran, et al., 2015). Several open-air sites have been discovered in the Central Alborz and the northern  
74 edge of the Iranian Central Desert: the Upper Paleolithic site of Garm Roud (Berillon et al., 2007, 2016)  
75 dated from the end of the MIS3, and the surface sites of Mirak (Rezvani, 1990; Vahdati Nasab et al. 2013),  
76 Moghanak and Otchunak (Berillon et al. 2007; Chevrier et al. 2006, 2010), Delazian (Vahdati Nasab and  
77 Clark, 2014), and Chah-e Jam (Vahdati Nasab and Hashemi 2016). The location and cultural affinities of  
78 these sites suggest that the northern fringes of the Iranian Central Desert could have constituted a  
79 corridor used during Upper Pleistocene hunter-gatherer dispersals (Vahdati Nasab et al., 2013).

80 In that chronocultural context, our interest focused on the open-air site of Mirak, which is located 16 km  
81 to the south of the outskirts of the city of Semnan (Fig. 2). First mentioned by Rezvani (1990), Mirak was  
82 officially surveyed in 2009 by one of the authors (HVN) as part of the Paleolithic Survey of the Iranian  
83 Central Desert Project (PSICDP) (Rezvani and Vahdati Nasab, 2010). This survey collected a large lithic  
84 assemblage from the surface of eight natural mounds with evident Middle Paleolithic affinities (flake-  
85 based blank production, an abundance of prepared and *chapeau de gendarme* platforms, a significantly  
86 high value for the Levallois index, the presence of tools typical of 'Mousterian' technology). Only scarce  
87 artifacts with Upper Paleolithic affinities were found at the site, which suggests either the presence of  
88 Upper Paleolithic techno-complex and/or the presence of transitional lithic industries at the site (Vahdati  
89 Nasab et al. 2013). Mound 8, though not the largest mound in Mirak, exhibits the greatest volume of lithic  
90 scatters on its surface and surroundings. Moreover, the presence of relatively dense archaeological  
91 material visible in spoil heaps around one of the clandestine looters' pits suggests some archaeological  
92 deposits of Middle and Upper Paleolithic affinities were still *in situ*, buried and protected by the mound.  
93 Based on the foregoing, there was a need for a systematic excavation in this vicinity. Based upon our  
94 preliminary observations, Mirak appeared to be potentially very informative. Therefore, three seasons of  
95 excavation at Mirak 8 were conducted under the framework of joint Iranian-French collaboration (May-  
96 June 2015, July-August 2016 and October-November 2017). The following presents the preliminary results  
97 of these excavations, concerning the nature of archaeological deposits at Mirak, their cultural affinities  
98 and their geological and absolute chronological framework. Finally, these original data provide new  
99 perspectives with regards to the human settlements of the region during the MIS3.

100

101

102 2. RESULTS AND DISCUSSION

103 2.1. THE EXCAVATION AND FINDS

104 The excavations at Mirak 8 exposed an area covering 36m<sup>2</sup> in total, divided between three main sectors  
105 (Fig. 3): 19 m<sup>2</sup> on the Northern slope of the mound, 12 m<sup>2</sup> on the Eastern slope and 5 m<sup>2</sup> on the Southern  
106 slope, delimited based on geoarchaeological prospecting. The excavation was carried out by squares with  
107 the surface area of 1 m<sup>2</sup> each, using both contextual and arbitrary level excavation techniques. The  
108 conventional 5 cm depth was adopted for each arbitrary archaeological level taking into account the  
109 depositional settings, and each excavated archaeological find was collected and referenced in the 3D  
110 frame of the mound. Dry and wet sieving of sediments were used when possible in order to sample micro-  
111 artifacts. The excavation exposed an excavated surface totaling 19 m<sup>2</sup> (North sector, 4 m<sup>2</sup>; East sector, 10  
112 m<sup>2</sup>; South sector, 5 m<sup>2</sup>).

113 The three campaigns of excavation yielded 6266 finds including 2709 objects precisely collected in the  
114 stratigraphic context and spread between 4 and 7 m below the top of the stratigraphic sequence. These  
115 archaeological materials are mainly composed of lithic artifacts (see below), but rare and extremely-  
116 altered fragments of bones and teeth of large mammals were also recovered; no sign of human  
117 intervention on these altered materials could be identified. The determinable teeth fragments belong to  
118 equids. No remains of small fauna were found either in excavation contexts or in the sieved sediments.

119 We focus here on the results of the excavation on the eastern trench where the archaeological density  
120 appeared to be the highest. Three main successive archaeological concentrations were clearly identified  
121 in stratigraphic context (Layers 1-3) (Fig. 5).

122

## 123 2.2. DEPOSITIONAL SETTING AND CHRONO-STRATIGRAPHIC FRAMEWORK OF MIRAK 8

### 124 2.2.1. The Mirak stratigraphic sequence

125 Mirak is located in a dry mudflat (53°25'53" E ; 35°28'10" N ; ca. 1035 masl) that extends from Semnan's  
126 piedmont along the southern flank of the Alborz Mountains to the northern edge of the Iranian Central  
127 Desert, also known as *Dasht-e Kavir*. This area belongs to an elongated Quaternary drainage system,  
128 which is characterized by alluvial fans and sedimentary pediments, with widespread saline playa-lake  
129 systems downstream.

130 Geomorphological fieldwork has revealed a pedo-sedimentary succession represented by a 9 m-thick  
131 alluvial-aeolian record made up of two main sequences (Sequence I: alluvial basal complex; Sequence II:  
132 windblown deposits) (see Fig. 4 for the synthetic stratigraphy and description). Sequence I can be divided  
133 into 6 lithostratigraphic units from the base upwards (Units 9-4; thickness: ca. 5 m). Horizontal bedding of  
134 silty clays (Units 8, 6 and 4) were observed in the stratigraphy. This stratigraphic column also includes at  
135 least two bodies of very fine sands (Units 7 and 5) and a deflated horizon (Unit 4a); these three units  
136 contain the three main archaeological assemblages (3 to 1 respectively). Sequence I accumulated on a  
137 pediplain that was flooded repeatedly as a consequence of shallow sheet flooding and channel overflows.  
138 Indeed, horizontal bedding prevails in the very fine sand units (Units 7 and 5), but current ripple marks  
139 and internal planar cross bedding occur as well (lithofacies Sr and Sp according to Miall 1996). The whole  
140 units are distinguished by intense post-depositional weathering resulting both from the repetition of  
141 decreases in the level of the water table and increases in the rate of evaporation as evidenced by Fe-Mn  
142 concretions, iron hydroxide precipitates, calcareous nodules, gypsum crystals and desiccation cracks.  
143 These features are associated to the development of 'Aridisol horizons' (Bk, By) (USDA, Soil Survey Staff,  
144 2014). The upper limit of this alluvial pedocomplex is marked by a major discontinuity, which corresponds  
145 to the contemporary deflation surface of *Dasht-e Kavir*. Sequence II of Mirak 8 mound can be divided into  
146 4 lithostratigraphic units from the base upwards (Units 3-0; thickness: about 4 m). The first part of this

147 sequence consists of calcareous aeolian sand deposits (Unit 3) reworked by a hydromorphic horizon (Unit  
148 2) top ward. The uppermost part of Sequence II is composed of another aeolian sand deposit (Units 1 and  
149 0) affected by the development of an Entisol (USDA).

150

### 151 2.2.2. Luminescence dating

152 Samples for luminescence dating were collected: six samples were taken from the northern section of  
153 Sequences I and II and two samples from the lower part of the eastern section of Sequence I . Preliminary  
154 dating results, including analytical data, are listed in Table 1 and plotted in their stratigraphic position in  
155 Fig. 4 (see also Supplementary Material for details on the implemented procedure). OSL and post-IR IRSL  
156 measurements were performed on multi-grain aliquots (See SM for methodological details). Overall, the  
157 OSL ages are coherent with the stratigraphy and the inter-aliquot dispersion in equivalent doses for each  
158 sample is very low; this allows us to consider the OSL ages to provide accurate, reliable ages. As a result,  
159 the ages range from  $50\pm 3$  to  $28\pm 2$  ka in the Sequence I that contains the three primary archaeological  
160 deposits, with a maximum age of  $28\pm 2$  ka for Layer 1, dates between  $28\pm 2$  and  $38\pm 2$  for Layer 2, dates  
161 between  $47\pm 2$  ka and  $47\pm 4$  ka for Layer 3(samples MK 16/2 and MK16/3), which correspond to the Last  
162 Glacial cycle. The ages range from  $1.2\pm 0.2$  to  $0.6\pm 0.1$  ka in Sequence II.

163

### 164 2.2.3. Formation of the mound of Mirak 8 and context of archaeological deposits

165 Based on the available data, it seems that Sequence I at Mirak Mound 8 may have formed as a response  
166 to climatic changes during the first half of the Last Glacial (probably during MIS 3), which was more humid  
167 than the Upper Pleniglacial (MIS 2 age equivalent). The records of these transitional periods are less well  
168 understood in the context of the northern Iranian paleoclimatic and chronostratigraphic framework for  
169 the Last Interglacial/Glacial cycle (*i.e.* the Lake Urmia core: Djamali et al., 2008 ; loess records of North of  
170 Iran: Kehl et al., 2005 and Frechen et al. 2009). Human occupations at Mirak were contemporaneous with

171 the aggradation of a covered pediment incised by anastomosed channels. This period was apparently  
172 characterized by rapid flooding events (*i.e.* sheet flood or crevasse splay deposits) that buried Paleolithic  
173 deposits. If the increase in rainfall events explains the accumulation of sediments deposited during flash  
174 floods, we do not exclude the influence of episodic uplift upstream as pointed out by Kehl (2009).  
175 Nevertheless, no stratigraphic evidence of tectonic effect has been observed. Aggradation of the alluvial  
176 cover ended with a major aridification marked by an aridisol development, perhaps indicating the end of  
177 the Last Glacial period. The scenario of a long-term drying coincided with a sedimentary hiatus, between  
178 the units 4 and 3, which, separated the Pleistocene desiccated flat from the Holocene sand dune  
179 (sequence II). The Holocene history of Mirak is defined by at least two phases of calcareous dust deposits  
180 interrupted by the temporary development of a perched water body on the first aeolian mound. The  
181 formation of this hydromorphic horizon (Unit 2) in arid environment implies a groundwater flux from the  
182 bedrock and its resurgence by a perched spring.

183 The study of the excavated sediments evidently indicates that in contrast to the current arid desert  
184 situation, the northern part of the Iranian Central Desert at least for the studied region had a completely  
185 different climate during the end of Pleistocene. During the first half of the Last Glacial Period (MIS 4/3)  
186 the climate of the region was cold and humid. This cold and humid period was characterized by a slow  
187 alluvial aggradation interrupted by rapid flooding events. Two of the archaeological layers at Mirak 8 are  
188 dated to the chronological interval between  $50 \pm 3$  ka and  $28 \pm 2$  ka, which corresponds to these humid  
189 climate conditions. Moreover, the different nature of sediments of the archaeological layers in  
190 comparison to the upper and lower sterile sediments implies that during each of these occupational  
191 events (which might have lasted hundreds of years), the site was situated on dry land, possibly surrounded  
192 by streams and marshes. Concerning the Holocene sequence (Sequence 2 in Mirak 8), the current study  
193 of Mirak 8 demonstrate that the mounds in Mirak cannot be seen as remnants of a more extensive deposit  
194 that has been eroded away but correspond to Holocene nebkha or shadow dunes. In Mirak 8, it results in

195 at least two phases of calcareous dust deposits interrupted by the temporary development of a perched  
196 water body on the first aeolian mound. The two OSL ages derived from the very top of the mound  
197 (MK15/1:  $0.6 \pm 0.1$ ka) and where the mound meets the flatland area around it (MK15/4:  $1.2 \pm 0.2$  ka)  
198 indicate that the formation of the mound of Mirak 8 took approximately 800-1600 years. Therefore, the  
199 mounds of the site were formed at a relative rapid pace. As mentioned above, such hydromorphic horizon  
200 in arid environment implies a groundwater flux from the bedrock and its resurgence by a perched spring.  
201 In that general pattern of dune formation, the vegetation may have played an important role in the  
202 formation of the mound by fixing the calcareous sands and consequently the preservation of the  
203 underlying Pleistocene sequence as originally proposed by Vahdati Nasab et al. (2013).

204

## 205 2.3. LITHICS AND CULTURAL AFFINITIES

### 206 2.3.1. The lithic assemblage

207 The lithic assemblage presented here consists of 2313 pieces from the easternmost excavation at Mirak  
208 8. More than 85% of these artifacts are made of varieties of chert (i.e. chert, flint, and jasper). Other raw  
209 materials are tuff, sandstone, siltstone, and rarely, microconglomerate. Within this assemblage, 976  
210 pieces are typologically indeterminable fragments or splinters most of which have very small dimensions  
211 and their techno-typological identification is problematic, if not impossible (see Jayez & Vahdati Nasab  
212 2016 for morphological characteristics of what is considered “indeterminable”). These pieces have been  
213 excluded from our analysis which leaves 1337 chipped stones to present, including 212 chips (Table 2)  
214 which are flakes mostly with less than 1 cm dimensions (see Shea, 2013: 32).

215 The three identified levels occurred in distinct stratigraphic units, although some vertical dispersion are  
216 observed within each level that may be related to some taphonomic agents (work in progress) (Fig. 5);  
217 however, the general state of preservation of the lithics is very good which testifies that, if taphonomy  
218 has impacted the deposits, the impact has been limited. In that respect, Level 1 appears to occur in a

219 deflated unit; this may explain the wider dispersion and lower density in objects than those observed for  
220 levels 2 and 3. In addition, few artefacts were located between these three main archaeological deposits,  
221 usually in roots whole or vertical breaks. Apart these very few pieces (around 30 among 2313 artefacts),  
222 the artefacts appear to depict three main archaeological deposit.

223

224 The L1 lithic assemblage appears to be an industry oriented toward a blade-bladelet production from at  
225 least carinated elements. No cores have been found and other tool types are underrepresented. Carinated  
226 burins are found exclusively in L1 (Fig. 6: 1-3) which are usually found in the so-called “Zagros Aurignacian”  
227 (see: Olszewski and Dibble, 1994, 2002) or “Baradostian” (see: Olszewski, 1993; Solecki, 1958) techno-  
228 complexes. The characteristic artifact-types of this assemblage include blades, bladelets, and their  
229 associated fragments (Fig. 6:4); although Arjeneh (Font-Yves) points and *lamelles Dufour* as major  
230 components of both Central Zagros and Southern Zagros Upper Paleolithic lithic industries (see Conard  
231 and Ghasidian, 2011; Ghasidian et al., 2017; Hole, 1970; Hole and Flannery, 1967; Otte et al., 2007) are  
232 not observed in the current assemblage of Mirak. Among the platform rejuvenation flakes in this  
233 assemblage is one large core tablet (Fig. 6: 5) which indicates the large dimensions of prismatic cores from  
234 which the blades were produced. Finally, Levallois-Mousterian tools are completely absent in this layer.  
235 As a whole, this layer shows Upper Paleolithic affinities. However, this assessment must be taken with  
236 caution; indeed, the density of artifacts is low (see Table 2) and the assemblage was preserved in a  
237 deflated horizon and thus may not be fully representative of the original one.

238 The L2 lithic assemblage is characterized by the mixed presence of Upper Paleolithic industries with  
239 characteristics of prismatic blade-bladelet production and Levallois-Mousterian flake-based production,  
240 the technological structure of which shows also a moderate percentage of cores and tools (Table 2). Few  
241 blades and bladelets are either plain or regularly retouched or notched (Table 4, Fig. 7: 4-5 ). Semi-parallel  
242 arrises (flake scar ridges) are present on the dorsal face of some blades (Fig. 7: 3). The Mousterian industry

243 artifact-types are dominated by the Levallois technique (for Mousterian artifact-types see e.g., Geneste,  
244 1985). They mostly indicate recurrent reduction strategy with radial/centripetal preparation (Fig. 7:6 ).  
245 Levallois flakes with faceted and *chapeau de gendarme* platforms are present as well as the byproducts  
246 of Levallois reduction strategy in the form of core preparation elements. Bladelets and some of the blades  
247 have been made via prismatic reduction method. It is worth mentioning that Levallois blade cores are rare  
248 in the Mirak assemblage. Regarding the tools (Table 4), among the interesting specimens is one elongated  
249 convergent blade with faceted striking platform and inverse notching/retouching (Fig. 7: 1 ). As a whole,  
250 Layer 2 appears to present a mix of characteristics usually associated with both Upper and the Middle  
251 Paleolithic industries.

252 In L3, cores and tools are well represented (twice as much as in upper layers). Most of the cores are  
253 Levallois cores (Fig. 8: 11). If the debitage composition of the layers is considered, L3 lithic assemblage,  
254 with less than 5% blade and bladelet products, indicates an industry based on flake production, a number  
255 of them being relatively elongated (Table 3). This assemblage includes Mousterian industry artifact-types  
256 similar to L2 with the dominance of Levallois technique with mostly recurrent reduction strategy with  
257 radial/centripetal preparation. Regarding the tools (Table 4), Levallois-Mousterian tools such as various  
258 scrapers (Fig.8: 8, 10) are present in high quantity in L3 as well as some points (Fig.8: 2, 5-7); they are  
259 comparable to those found in the Zagros Mousterian (see Dibble, 1993; Dibble and Holdaway, 1993;  
260 Lindly, 1997). Some tools have basal trimming which might be attributed to the hafting methods (Fig. 8:  
261 1, 8). There are also Levallois points with retouch on both faces and faceted striking platform (Fig. 7: 9).  
262 As a whole, L3 has clear Middle Paleolithic affinities.

263 However, the vertical distribution and field data (such as postdepositional reworking) shows that some  
264 pieces cannot be precisely allocated to Layers 2 or 3; among these pieces, one carinated scraper as well  
265 as a prismatic core (Fig. 8: 3), here vertical between L2 and L3 respectively, are usually considered as a

266 typical implement of Upper Paleolithic industry of Baradostian/Zagros Aurignacian (see Olszewski and  
267 Dibble, 2006; Otte et al., 2007).

268

### 269 **2.3.2.** Phases of human occupation

270 In contrast to what has been claimed previously about the Middle Paleolithic affinities based on the study  
271 of the surface collection of the lithic industries in Mirak (Rezvani and Vahdati Nasab, 2010; Vahdati Nasab  
272 et al., 2013), the data derived from the three seasons of excavations at Mirak 8 has clearly identified the  
273 presence of vestiges of at least three main archaeological layers.

274 The upper layer, i.e. L1, has clear Upper Paleolithic affinities, with some resemblance (carinated burins)  
275 with the so-called “Zagros Aurignacian” (Olszewski and Dibble, 1994, 2002) or “Baradostian” (Olszewski,  
276 1993; Solecki, 1958) techno-complexes. Yet Arjeneh (Font-Yves) points and *lamelles Dufour* as major  
277 components of both Central Zagros and Southern Zagros Upper Paleolithic lithic industry (see Conard and  
278 Ghasidian 2011; Ghasidian et al., 2017; Hole, 1970; Hole and Flannery, 1967; Otte et al., 2007) are not  
279 observed in the current assemblage of Mirak; if confirmed, Mirak would more closely resembles Garm  
280 Roud, which dates to around 33 kya (Berillon et al., 2007, 2016; Chevrier et al., 2006). However, the low  
281 density of artifacts in L1 and its evident reworked nature does not allow a precise determination of this  
282 upper assemblage and needs caution in its interpretation. The Upper Paleolithic affinities are consistent  
283 with the OSL dating that gives a maximum age of  $28\pm 2$  kya and with the presence of a large Upper  
284 Paleolithic open-air site, i.e. Delazian, at a very close proximity (2km northeast of Mirak, see Vahdati Nasab  
285 and Clark, 2014).

286 The lower layer, i.e. L3, has clear Middle Paleolithic affinities; with regards to Levallois-Mousterian tools  
287 (various scrapers and points), the assemblage is comparable to those of classical Zagros Mousterian sites  
288 (see Dibble, 1993; Dibble and Holdaway, 1993; Lindly, 1997). Interestingly, this assemblage dates between  
289  $47\pm 2$  kya and  $47\pm 4$  kya, which although compatible with the general chronological framework of Middle

290 Paleolithic assemblages in the Middle East, appears very recent compared to the Middle Paleolithic known  
291 in the Zagros, and earlier than the early Upper Paleolithic assemblages of the Zagros (Becerra-Valdivia et  
292 al., 2017).

293 The intermediate layer, i.e. L2, might be the most controversial one, representing a mixture of industries  
294 with both Middle and Upper Paleolithic affinities, in a chronological framework that dates it between  $28\pm 2$   
295 and  $38\pm 2$  kya. Based on this preliminary chronological framework, L2 appears possibly contemporary from  
296 the Early Upper Palaeolithic of the Zagros (Becerra-Valdivia et al., 2017), where faceted platforms or  
297 sidescrapers have been identified (e.g. Tsanova, 2013). However, more studies are ongoing, including the  
298 technotypology of the intermediate layer, as well as a refined chronology based on recent OSL samples  
299 that should allow us refining our understanding of the nature, the chronology and the context of this  
300 intermediate human occupations at Mirak. However, to our knowledge, despite some potential  
301 resemblances with the Early Upper Palaeolithic of the Zagros, such mixture of industries has no equivalent  
302 to date within the regional context of the Iranian Central Plateau, and together with its chronological  
303 framework points the complexity of the cultural evolution in a wide area between Zagros and Central Asia.  
304 Finally, beside this general pattern, a carinated scraper and a prismatic core which are typical of the  
305 Baradostian/Zagros Aurignacian (see Olszewski and Dibble, 2006; Otte et al., 2007) have been collected  
306 between the lowest layers (L2 and L3) and could not be allocated precisely to one of these levels.  
307 Although, as mentioned above, this may be related to some post-depositional reworking based on field  
308 data and vertical distribution, this points to the originality of the lithic industries of Mirak, and one cannot  
309 exclude some potential affinities of the Mirak's lower lithic assemblages with early Upper Paleolithic or  
310 late Middle Paleolithic cultures of the Zagros. Further analysis of the lithic assemblage will address these  
311 potential affinities.

312

313 **3. CONCLUSION**

314 In summary, Mirak provides unique data in the area between the Zagros and Central Asia, depicting  
315 successive phases of human occupation in the Iranian Central Plateau during the late Pleistocene,  
316 anchored in a precise geological and chronological framework, in contrast to previous studies, which had  
317 relied solely on surface finds. Although caution is needed, from the lithics analysis and the distribution of  
318 the finds, at least three main archaeological layers can be identified in Mirak 8. These layers appear to be  
319 culturally and chronologically distinct, corresponding to at least three main phases of human occupation.  
320 The upper layer (L1) with a maximum age of 28kya, shows some Upper Paleolithic affinities, although  
321 poorly preserved. The intermediate layer (L2) indicates characteristics similar to both Upper and Middle  
322 Palaeolithic industries that can be seen as an intermediate Paleolithic and dates between 28±2 and 38±2  
323 kya; it appears very original in the Iranian Central Plateau context. The lower layer (L3) has clear Middle  
324 Paleolithic affinities and dates around 47kya; it would represent a very recent Middle Palaeolithic industry  
325 compared to what is known in the area. Although further investigations are needed and in progress, Mirak  
326 industries points the complexity of the cultural evolution in a wide area between Zagros and Central Asia.

327

328

329

330 **ACKNOWLEDGMENTS**

331 We would like to thank the Research Center for Cultural Heritage and Tourism of Iran (RICHT) and the  
332 Iranian Center for Archaeological Research (ICAR) for granting us the permit to conduct the fieldworks at  
333 the site. We also would like to express our great gratitude to Mr. Jalil Golshan at the RICHT for his  
334 tremendous support during the three seasons of the field missions. We thank the Office of International  
335 Affairs at the RICHT for facilitating the process of visa for the non-Iranian partners of the project. We are

336 greatly indebted to Mr. Khajeh Beidokhti, the director of the Iranian Cultural Heritage Organization (ICHO)  
337 office in Semnan Province and his colleagues for providing such ideal conditions to conduct the fieldwork.  
338 The fieldwork and geological analyses have been cofounded by the office of governor of Semnan (Dr.  
339 Khabbaz and his deputy Mr. Zandieh Vakil), the French Ministry of Europe and Foreign Affairs (MEAE) and  
340 the UMR7194 CNRS-MNHN-UPVD (Paris); we are very grateful to them. The luminescence dating study  
341 was conducted thanks to financial support from the French National Research Agency via the LaScArBx  
342 Labex (Project number ANR-10-LABX-52). We would also like to thank Patrick August for his help in  
343 identification of the fauna remains. Mr. Hassan Rezvani, the discoverer of Mirak, generously allowed us  
344 to conduct field research there. We are grateful to Mr. Soroush Hashemi, and Kamran Shojaee at the ICHO  
345 office in Semnan for their magnificent logistical support. Dr. Kourosh Mohammadkhani assisted us in  
346 geomagnetic fieldwork. Dr. Razieh Lak, Research Deputy at the Geological Survey of Iran and Mr. Habib  
347 Poorfaraj who was in charge of the raw material sourcing, we thank all of them. We are grateful to Mr.  
348 Iraj Beheshti at the Iranian Centre for Preservation and Restoration, for his help in identifying the raw  
349 material types. We would like to thank Kyle G. Olson for his help in editing the final manuscript.  
350 Contributions of co-authors: responsibilities (HVN, GB, AAK), lithics analysis (MiH, MJ, SB), fauna (NS, ZA),  
351 geology (GJ, MAK), chronology (GG, MaH), spatial distribution (GB and MiH), design (HVN, GB) and writing  
352 of the manuscript (all).

353 Special thanks go to the field crew in alphabetical order: Alieh Abdollahi, Mahkameh Abolfathi, Laya Alinia,  
354 Benoit Chevrier, Nasim Feizi, Mahyar Khademi, Ashghar Nateghi, Mona Oryat, Soroush Razi, Robabeh  
355 Sadeghinejad, Yashar Sadeghi, Sanaz Shirvani, Mohammad Javad Shojaee, and Marzieh Zareh Khalili.

356

357

358 REFERENCES

359 Bazgir, B., Otte, M., Tumung, L., Ollé, A., Ganesh Deo, S., Joglekar, P., López García, M.J., Picin, A., Davoudi,  
360 D., Van Der Made, J., 2014. Test excavations and initial results at the Middle and Upper Paleolithic sites  
361 of Gilvaran, Kaldar, Ghamari caves and Gar Arjene rockshelter, Khorramabad Valley, Western Iran.  
362 *Comptes Rendus Palevol.* 13(6), 511-525.

363

364 Bazgir, B., Ollé, A., Tumung, L., Becerra-Valdivia, L., Douka K., Higham, T., van der Made, J., Picin, A.,  
365 Saladié, P., López-García, J.M. et al., 2017. Understanding the emergence of modern humans and the  
366 disappearance of Neanderthals: Insights from Kaldar Cave (Khorramabad Valley, Western Iran). *Nature*  
367 *Scientific Reports.* 7, 43460.

368

369 Becerra-Valdivia, L., Douka, K., Comeskey, D., Bazgir, B., Conard, N.J., Marean, C.W., Ollé, A., Otte, M.,  
370 Tumung, L., Zeidi, M., et al., 2017. Chronometric investigations of the Middle to Upper Paleolithic  
371 transition in the Zagros Mountains using AMS radiocarbon dating and Bayesian age modelling. *Journal of*  
372 *Human Evolution.* 109, 57-69.

373

374 Berillon, G., Asgari Khaneghah, A., Antoine, P., Bahain, J.J., Chevrier, B., Zeitoun, V., Aminzadeh, N.,  
375 Beheshti, M., Ebadollahi Chanzangh, H., Nochadi, S., 2007. Discovery of new open-air Paleolithic localities  
376 in Central Alborz, Northern Iran. *Journal of Human Evolution.* 52, 380-387.

377

378 Berillon G., Asgari Khaneghah A. (dir.) with the collaboration of Antoine P., Auguste P., Bahain J.-J.,  
379 Chausse C., Chevrier B., Ghaleb B., Jolly-Saad M.-C., Klaus S., Lebreton V., Limondin-Lozouet N., Mercier

380 N., Senegas F., Vahdati Nasab H., Vercoutere C., Zeitoun V. 2016. Garm Roud: A Hunting place in Iran,  
381 Upper Paleolithic. Editions IFRI & Archéo-éditions (French-English-Persian).  
382

383 Biglari, F., 2000. Recent finds of Paleolithic period from Bisotun, Central Western Zagros Mountains,  
384 Iranian Journal of Archaeology and History. Serial 28, 14(2), 50-60 (in Persian).

385 Biglari, F., Javeri, M., Mashkour M., Yazdi, M., Shidrang, S., Tengberg, M., Taheri, K., Darvish, J., 2009. Test  
386 excavations at the Middle Paleolithic sites of Qaleh Bozi, Southwest of Central Iran, A preliminary report,  
387 in: Otte, M., Biglari, F., Jaubert, J. (Eds.), Iran Paleolithic / Le Paléolithique d'Iran. UISPP, Proceedings of  
388 the XV World Congress (Lisbon, 4-9 September 2006). Oxford, BAR S1968, pp.29-38.

389

390 Braidwood, R., Howe, B., 1961. The Iranian Prehistoric Project. Science 133:2008–10. In: Marean, C. W.,  
391 & Kim, S. Y. (1998). Mousterian large-mammal remains from Kobeh Cave behavioral implications for  
392 Neanderthals and early modern humans. Current Anthropology. 39(S1), S79-S114.

393

394 Chevrier, B., Berillon, G., Asgari Khaneghah, A., Antoine, P., Bahain, J.-J., Zeitoun, V., 2006. Moghanak,  
395 Otchounak, Garm Roud 2: nouveaux assemblages paléolithiques dans le Nord de l'Iran. Caractérisations  
396 typo-technologiques et attributions chrono-culturelles. Paléorient. 32, 59-79.

397

398 Conard, N.J., Ghasidian, E., 2011. The Rostamian cultural group and the taxonomy of the Iranian Upper  
399 Paleolithic, in: Conard, N.J., Drechsler, P., Morales, A. (Eds), Between Sand and Sea. The Archaeology and  
400 Human Ecology of Southwestern Asia. Kerns Verlag, 744.Tübingen, pp. 33-52.

401

402 Coon, C. S., 1951. Cave Explorations in Iran 1949, Museum Monographs, the University Museum,  
403 University of Pennsylvania: Philadelphia.

404

405 Dibble, H.L., 1993. Le Paléolithique moyen récent du Zagros. Bulletin de la Société préhistorique française.  
406 90(4): 307-312.

407 Dibble, H.L., Holdaway, S.J.. 1993. The Middle Paleolithic Industries of Warwasi, in: Olszewski, D.I., Dibble,  
408 H.L. (Eds.), The Paleolithic Prehistory of the Zagros-Taurus. Philadelphia, University of Pennsylvania,  
409 University of Museum Symposium Series. 5, 75-99.

410

411 Djamali, M., de Beaulieu, J.-L., Shah-hosseini, M., Andrieu-Ponel, V., Ponel, P., Amini, A., Akhani, H., Leroy,  
412 S.A.G., Stevens, L., Lahijani, H. and S. Brewer. 2008. A late Pleistocene long pollen record from Lake Urmia,  
413 Iran. Quaternary Research. 69, 413-420.

414

415 Frechen, M., Kehl, M., Rolf, C., Sarvati, R. and A. Skowronek. 2009. Loess chronology of the Caspian  
416 Lowland in Northern Iran. Quaternary International. 198, 220-233.

417

418 Geneste, J.-M., 1985. Analyse lithique d'industries moustériennes du Périgord: approche technologique  
419 du comportement des groupes humaine au Paléolithique moyen. PhD thesis, University of Bordeaux.

420

421 Ghasidian, E., Bretzke K., Conard, N. J., 2017. Excavations at Ghar-e Boof in the Fars Province of Iran and  
422 its Bearing on Models for the Evolution of the Upper Paleolithic in the Zagros Mountains. Journal of  
423 Anthropological Archaeology. 47, 33-49.

424

425 Heydari, S., A. Azadi, Ghasidian, E., 2004. Paleolithic survey in Southwestern Zagros, Basht Valley.  
426 Unpublished manuscript, Iranian Center for Archaeological research, Tehran, Iran. (in Persian).

427

428 Heydari-Guran, S., Ghasidian, E., 2017. The MUP Zagros Project: tracking the Middle Upper Paleolithic  
429 transition in the Kermanshah region, west-central Zagros, Iran. *Antiquity*. 91(355), 1-7.

430 Hole, F., 1970. The Paleolithic Culture Sequence in Western Iran. *Proceedings of the VIIth International*  
431 *Congress of Prehistoric and Protohistoric Sciences, Prague*, pp. 286-292.

432

433 Hole, F., Flannery, K., 1967. The Prehistory of South-western Iran: a preliminary report. *Proceedings of*  
434 *Prehistory Society*. 38, 147-206.

435

436 Jaubert, J., Biglari, F., Mourre, V., Bruxelles, L., Bordes, J.-G., Shidrang, S., Naderi, R., Mashkour, M.,  
437 Maureille, B., Mallye, J.-B., Quinif, Y., Rendu, W., Laroulandie, V., 2009. The Middle Paleolithic occupation  
438 of Mar-Tarik, a new Zagros Mousterian site in Bisotun massif (Kermanshah, Iran), in: Otte, M., Biglari, F.,  
439 Jaubert, J. (Eds.), *Iran Paleolithic / Le Paléolithique d'Iran*. UISPP, *Proceedings of the XV World Congress*  
440 *(Lisbon, 4-9 September 2006)*. Oxford, BAR S1968, p. 7-27.

441

442 Jaubert, J., Biglari, F., Crassard, R., Mashkour, M., Rendu, W., Shidrang, S., 2008. Paléolithique moyen  
443 récent de la grotte de Qaleh Bozi 2 (Ispahan, Iran): premiers résultats de la campagne 2008. *Journal of*  
444 *iranian archaeology, Šahrām Zāri*. 2010, 21-31.

445

446 Kehl, M., 2009. Quaternary climate change in Iran—the state of knowledge. *Erkunde*. 63, 1-17.

447

448 Kehl, M., Sarvati, R., Ahmadi, H., Frechen, M., Skowronek, A., 2005. Loess paleosol-sequences along a  
449 climatic gradient in Northern Iran. *Eiszeitalter u. Gegenwart*. 55, 149-173.

450

451 Lindly, J.M., 2005. The Mousterian of the Zagros: a regional perspective. Tempe: Arizona State University  
452 Anthropological Research Papers.

453 McBurney, C.B.M., 1964. Preliminary Report on Stone Age Reconnaissance in north-eastern Iran.  
454 Proceedings of the Prehistoric Society. 16, 382-399.

455

456 Olszewski, D. I., 1993. The Zarzian Occupation at Warwasi Rockshelter, Iran, in: Olszewski, D.I., Dibble, H.L.  
457 (Eds.), The Paleolithic Prehistory of the Zagros-Taurus. Philadelphia, University of Pennsylvania, University  
458 of Museum Symposium Series. 5, 207-236.

459

460 Olszewski, D.I., Dibble, H., 1994. The Zagros Aurignacian. *Current Anthropology*. 35, 68-75.

461

462 Olszewski, D.I., Dibble, H., 2006. To be or not to be Aurignacian: The Zagros Upper Paleolithic, in Bar-Yosef,  
463 O., Zilhao, J. (Eds.), *Toward a Definition of the Aurignacian*. Oxford, Oxbow Books, pp. 355-373.

464

465 Otte, M., and Biglari, F. 2004. Témoins aurignaciens dans le Zagros, Iran. *Anthropologie (1962-)*, 42(3),  
466 243-248.

467

468 Otte, M., Biglari, F., Flas, D., Shidrang, S., Zwyns, N., Mashkour, M., Naderi, R., Mohaseb, A., Hashemi, N.,  
469 Darvish, J., Radu, V., 2007. The Aurignacian in the Zagros Region: New Research at Yafteh Cave, Lorestan,  
470 Iran. *Antiquity*. 81, 82-96.

471

472 Otte, M., Biglari, F., Jaubert, J., 2009. Iran Paleolithic / Le Paléolithique d'Iran. UISPP, Proceedings of the  
473 XV World Congress UISPP (Lisbon, 4-9 September 2006). Oxford, BAR International Series, S1968, 157 p.

474 Otte, M., Shidrang, S., Zwyns, N., Flas, D., 2011. New radiocarbon dates for the Zagros Aurignacian from  
475 Yafteh cave, Iran. *Journal of Human Evolution*. 61(3), 340-346.  
476

477 Otte, M., Shidrang, S., Flas, D., 2012. The Aurignacian of Yafteh Cave and Its Context (2005–2008  
478 excavations). *ERAUL* 132.  
479

480 Rezvani, H., 1990. Settlement patterns of prehistoric cultures in Semnan. in: Alizadeh, A., Majidzadeh, Y.,  
481 Malek Shahmirzadi, S. (Eds), *Thirty-two Essays in Memory of E. Negahban*. Tehran, Tehran University  
482 Press, pp. 7-19.  
483

484 Rezvani, H, Vahdati Nasab, H., 2010. A major Middle Paleolithic open site at Mirak, Semnan Province, Iran.  
485 *Antiquity* 84 (323): Project Gallery December 2009 (<http://antiquity.ac.uk>).  
486

487 Roustaei, K., Biglari, F., Heydari, S., Vahdati Nasab, H., 2004. New Research the Paleolithic of Lorestan,  
488 West Central Iran. *Antiquity*. 76, 19–20.  
489

490 Shea, J.J., 2013. *Stone Tools in the Paleolithic and Neolithic Near East: A Guide*. Cambridge University  
491 Press.  
492

493 Shidrang, S., Biglari, F., Bordes, J. G., Jaubert, J., 2016. Continuity and change in the late Pleistocene lithic  
494 industries of the central Zagros: a typo-technological analysis of lithic assemblage from Ghar-e Khar cave,  
495 Bisotun, Iran. *Archaeology, Ethnology and Anthropology of Eurasia*. 44/1 (2016) 27–38.  
496

497 Smith, P.E.L., 1986. *Paleolithic Archaeology in Iran*. Philadelphia: The University Museum.

498

499 Soil Survey Staff, 2014. Keys to Soil Taxonomy, 12th ed. Washington, DC.: USDA-Natural Resources  
500 Conservation Service.

501 Solecki, R. S. 1955. *Shanidar cave: a paleolithic site in northern Iraq* (pp. 389-425). Smithsonian Institution.

502

503 Solecki, R., 1958. The Baradostian Industry and the Upper Paleolithic in the Near East. PhD Dissertation,  
504 Columbia University.

505

506 Tsanova, T., 2013. The beginning of the Upper Paleolithic in the Iranian Zagros. A taphonomic approach  
507 and techno-economic comparison of Early Baradostian assemblages from Warwasi and Yafteh (Iran).  
508 *Journal of Human Evolution*. 65(1), 39-64.

509

510 Vahdati Nasab, H, Clark, G.A., 2014. The Upper Paleolithic of the Iranian Central Desert: the Delazian Sites,  
511 Semnan Province – a Case Study. *Archaeologische Mitteilungen aus Iran und Turan (AMIT)*. 46, 1-21.

512

513 Vahdati Nasab, H, Hashemi, M., 2016. Playas and Middle Paleolithic settlement of the Iranian Central  
514 Desert: The discovery of the Chah-e Jam Middle Paleolithic site. *Quaternary International*. 408, 140-152.

515

516 Vahdati Nasab, H, Clark, G.A., Torkamandi, S., 2013. Late Pleistocene dispersal corridors across the Iranian  
517 Plateau: A case study from Mirak, a Middle Paleolithic site on the northern edge of the Iranian Central  
518 desert (Dasht-e Kavir). *Quaternary International*. 300, 267-281.

519

520 Young, C. T, Smith, P., 1966. Research in the prehistory of Central Western Iran. *Science*. 153, 386-391.

521

522 Zander, A., Hilgers, W., 2013. Potential and limits of OSL, TT-OSL, IRSL and pIRIR<sub>290</sub> dating methods applied  
523 on a Middle Pleistocene sediment record of Lake El'gygytgyn, Russia. *Climate of the Past*. 9, 719-733.

524

525 Zeitoun, V., 2016. Where palaeoanthropology and prehistory meet, in: Berillon, G., Asgari-Khaneghah, A.  
526 (Eds), *Garm Roud. A Hunting place in Iran, Upper Paleolithic*. Paris, Editions IFRI & @rchéo-éditions, pp.  
527 101-110.

528

529 FIGURES' CAPTIONS:

530 Figure 1. Map of some of the major Paleolithic sites in the studied area / Carte des sites paléolithiques  
531 majeurs de la région d'étude

532

533 Figure 2. Northern Iranian Central Desert and Mirak 8 / Le Nord du désert central iranien et la bute  
534 Mirak 8

535

536 Figure 3. Topographic map of Mirak 8 / Carte topographique de Mirak 8

537

538 Figure 4. Synthetic stratigraphy of Mirak 8 in 2016 and location of the OSL/IRSL dating. 0. Topsoil with  
539 platy structure (*vegetalized surface of the mound*); 1. Light brown sandy silt with massive structure  
540 (*Entisol developed on calcareous windblown deposits*); 2. Convoluted light grey sandy silt including  
541 lenses of reworked wind-blown deposits (unit 1) (*hydromorphic horizon*); 3. Brown clayey silt with  
542 massive structure (*calcareous windblown deposits*); 4a. Pale green silty clay with polyhedral structure  
543 (*non-calcareous floodplain fines - hydromorphic horizon*); 4b and 6. Greyish green silty clay with  
544 prismatic structure and Fe-Mn oxide coatings (*non-calcareous floodplain fines*); 5 and 7. Pale green silty  
545 sand with current ripples (Sr) and internal planar crossbedding (Sp) (*shallow water deposits and minor*

546 *channel fills*); 8. Dark greyish green silty clay with prismatic structure including Fe-Mn oxide coatings,  
547 very fine sands and small pebbles of grey sandstone (*non-calcareous floodplain fines and crevasse splay*  
548 *deposits*); 9. Dark brown silty clay (Sketch by G.Jamet). This synthetic stratigraphy was built up on the  
549 basis of the correlation between three vertical sections (North, East & South trenches) and 14 sediment  
550 logs from auger surveys and clandestine holes.

551 Stratigraphie synthétique de Mirak 8 (2016) et localisation des âges OSL/IRSL. 0. sol arable à structure  
552 plate (surface végétalisée de la butte) ; 1. silt sableux brun clair à structure massive (Entisol développé  
553 sur des dépôts calcaires soufflés par le vent) ; 2. silt sableux gris clair volumineux comprenant des  
554 lentilles de dépôts remaniés par le vent (unité 1) (horizon hydromorphique) ; 3. silt argileux brun à  
555 structure massive (dépôts calcaires soufflés au vent) ; 4a. Argile silteuse vert pâle à structure  
556 polyédrique ; 4b et 6. Argile silteuse vert grisâtre à structure prismatique et revêtements d'oxyde de Fe-  
557 Mn ; 5 et 7. Sable silteux vert pâle avec des ondulations de courant (Sr) et lits entrecroisés planaires  
558 internes (Sp) (dépôts d'eau peu profonds et remplissages mineurs des chenaux) ; 8. argile silteuse vert  
559 grisâtre foncé à structure prismatique comprenant des revêtements d'oxyde de FeMn, du sable très fin  
560 et de petits cailloux de grès gris (dépôts fins et craquellés non calcaires de plaine d'inondation) ; 9. argile  
561 limoneuse brun foncé (dessin de G. Jamet). Cette stratigraphie synthétique a été construite sur la base  
562 de la corrélation entre trois sections verticales (tranchées Nord, Est et Sud) et 14 diagraphies  
563 sédimentaires provenant de levés à la tarière et de sondages clandestins.

564

565 Figure 5. Mirak 8 - Vertical distribution of the archaeological finds, Eastern sector; pecks of high density  
566 (black arrows). The projection of finds in the East-West vertical plane highlights the three main  
567 archaeological concentrations observed during the excavation. They represent a sub-horizontal slope,  
568 with a slight dip upwards near the periphery of the mound. The upper assemblage depth (L1) is around  
569 100 +/- 20 cm above the reference level. The intermediate assemblage (L2) is the thickest with a depth

570 around 20 +/- 30 cm below the reference level. The basal assemblage (L3) is around 115 +/- 12 cm below  
571 the reference level.

572 Mirak 8 - Distribution verticale des objets archéologiques, Secteur Est ; pics de densité (flèches noires).  
573 La projection des objets dans le plan vertical est-ouest met en évidence les trois principales  
574 concentrations archéologiques observées lors des fouilles. Subhorizontale, vers l'ouest, elles présentent  
575 un léger pendage vers le haut près de la périphérie du monticule. L'assemblage supérieur (L1) est à  
576 environ 100 +/- 20 cm au-dessus du niveau de référence. L'assemblage intermédiaire (L2) est le plus  
577 épais, à une profondeur d'environ 20 +/- 30 cm en dessous du niveau de référence ; au centre de la butte  
578 (lignes O & P). L'assemblage profond (L3) est à environ 115 +/- 12 cm sous le niveau de référence.

579

580 Figure 6. Lithic artifacts from L1. 1-3. Carinated burin ; Twisted blade ; 5. Core tablet (drawings by M.  
581 Jayez).

582 Industrie lithique de L1. 1-3. Burins carénés ; 4. Lame torse ; 5. Tablette (dessins de M. Jayez).

583 Figure 7. Lithic artifacts from L2. 1. Mousterian point on Blade ; 2. End scraper ; 3-4. Bladelet fragments ;  
584 5. Notched blade fragment ; 6 Recurrent centripetal flake core (drawings by M. Jayez).

585 Industrie lithique de L2. 1. Pointe moustérienne sur lame ; 2. Grattoir terminal ; 3-4. Fragments de  
586 lamelles ; 5. Fragment de lame avec encoche ; 6. Nucléus récurrent, centripète à éclats, (dessins de M.  
587 Jayez).

588 Figure 8. Lithic artifacts from L3. 1. Notch-denticulated ; 2. Convergent point/scrapper ? 3. Prismatic core  
589 (L2-L3) ; 4. Levallois Blade ; 5. Déjeté point; 6-7. Mousterian point on elongated flake; 8. End scraper  
590 with basal trimming on the ventral face; 9. Levallois point ; 10. Side scraper and notched ; 11. Levallois  
591 flake core (drawings by M. Jayez).

592 Industrie lithique de L3. 1. Denticulé; 2. Pointe/grattoir? convergent 3. Nucleus prismatique (L2-L3) ; 4.  
593 Lame Levallois ; 5. Pointe déjetée ; 6-7. Pointes moustériennes sur éclat allongé ; 8. Grattoir terminal

594 avec retouche basale sur la face ventrale ; 9. Pointe levallois ; 10. Grattoir latéral et encoche ; 11.

595 Nucleus levallois à éclat (dessins de M. Jayez).

596

597

Table 1. Summary of quartz OSL and feldspar Post-IR IRSL data

Sample	Depth* (m)	Quartz OSL				Feldspar post-IR IRSL			
		n	D <sub>e</sub> (Gy)	Dose rate (Gy.ka <sup>-1</sup> )	Age (ka)	n	D <sub>e</sub> (Gy)	Dose rate (Gy.ka <sup>-1</sup> )	Age (ka)
MK15/1	0.65	20	1.2±0.2	2.18±0.05	0.6±0.1	15	4.4±0.3	2.51±0.07	1.7±0.1
MK15/4	3.50	18	2.9±0.4	2.39±0.04	1.2±0.2	15	7.6±0.3	2.72±0.07	2.8±0.1
MK15/5	4.10	25	92±4	3.29±0.07	28±1	15	118±4	3.62±0.09	32±2
MK15/6	4.55	25	95±6	3.37±0.06	28±2	14	116±3	3.70±0.08	31±1
MK15/8	5.70**	25	135±6	3.60±0.05	38±2	14	197±4	3.93±0.07	50±2
MK15/7	6.20	25	159±6	3.16±0.09	50±3	14	249±9	3.49±0.10	71±4
MK16/2	-1.10	19	123±4	2.63±0.08	47± 2	15	193±8	2.99±0.08	65± 4
MK16/3	-1.18	20	156±11	3.32±0.10	47±4	15	454±52	3.68±0.10	123±17

599

600 \* compared to the top of the stratigraphy

601 \*\* MK15/8, sampled in S2 at 4.60m below the top of the S2 stratigraphy

602 **Notes.** 'D<sub>e</sub>' is the average equivalent dose and 'n' is the number of measured aliquots.

603

604 Table 2. Technological Structure of Mirak Chipped Stone Assemblage (L=Layer; Lithic density=total  
605 quantity of chipped stones/excavated volume in m<sup>3</sup>)

	L1	%	L2	%	L3	%	Sum
<b>Core and frags</b>	0	<b>0</b>	12	<b>1.8</b>	27	<b>4.2</b>	39
<b>Tools</b>	10	<b>18.2</b>	121	<b>18.7</b>	225	<b>35.5</b>	356
<b>Debris</b>	0	<b>0</b>	13	<b>2</b>	12	<b>1.9</b>	25
<b>Debitage</b>	45	<b>81.8</b>	502	<b>77.5</b>	370	<b>58.4</b>	917

<b>Sum</b>	<b>55</b>	<b>100</b>	<b>648</b>	<b>100</b>	<b>634</b>	<b>100</b>	<b>1337</b>
+Indeterminable Fragments	13		496		467		<del>976</del>
Lithic density	9.5		101.7		237.8		<del>1008</del>

609

610

611

612

613

614

615

Table 3. Debitage composition of Mirak Chipped Stone Assemblage (L=Layer)

616

617

Debitage	L1	%	L2	%	L3	%	Sum
<b>Bladelets and Fragments</b>	4	8.9	21	4.2	4	1.1	29
<b>Blades and Fragments</b>	3	6.7	41	8.2	15	4.1	59
<b>Flakes and Fragments</b>	33	73.3	326	64.9	258	69.7	617
<b>Chips</b>	5	11.1	114	22.7	93	25.1	212
<b>Sum</b>	<b>45</b>	<b>100</b>	<b>502</b>	<b>100</b>	<b>370</b>	<b>100</b>	<b>917</b>

623

624

625

Table 4. Tools composition of Mirak Chipped Stone Assemblage (L=Layer)

Tool Type	L1	%	L2	%	L3	%	Sum	%
<b>Flake Tools:</b>								
<b>Multiple Tools</b>	<b>1</b>	<b>10</b>	<b>5</b>	<b>4.1</b>	<b>13</b>	<b>5.8</b>	<b>19</b>	<b>5.3</b>
Scraper and Notched	0		5		12		17	

	Scraper and Burin	0	0	1	1				
	Scraper and Carinated Burin	1	0	0	1				
<b>Retouched</b>		<b>3</b>	<b>30</b>	<b>30</b>	<b>24.8</b>	<b>56</b>	<b>24.9</b>	<b>89</b>	<b>25.0</b>
<b>Burin</b>		<b>2</b>	<b>20</b>	<b>1</b>	<b>0.8</b>	<b>3</b>	<b>1.3</b>	<b>6</b>	<b>1.7</b>
	Simple	0	0	3	3				
	Transverse	0	1	0	1				
	Carinated	2	0	0	2				
<b>Notch-Denticulated</b>		<b>2</b>	<b>20</b>	<b>17</b>	<b>14</b>	<b>37</b>	<b>16.4</b>	<b>56</b>	<b>15.7</b>
<b>Scraper</b>		<b>2</b>	<b>20</b>	<b>37</b>	<b>30.6</b>	<b>89</b>	<b>39.6</b>	<b>128</b>	<b>36.0</b>
	Double	1	3	13	17				
	Side	1	19	50	70				
	End	0	9	6	15				
	Convergent	0	6	11	17				
	Déjeté	0	0	5	5				
	Round	0	0	2	2				
	Carinated	0	0	1	1				
	Transverse	0	0	1	1				
<b>Point</b>		<b>0</b>	<b>0</b>	<b>9</b>	<b>7.5</b>	<b>6</b>	<b>2.7</b>	<b>15</b>	<b>4.2</b>
	Levallois	0	3	2	5				
	Mousterian	0	6	3	9				
	Déjeté	0	0	1	1				
<b>Blade Tools:</b>		<b>0</b>	<b>0</b>	<b>16</b>	<b>13.2</b>	<b>17</b>	<b>7.5</b>	<b>33</b>	<b>9.3</b>

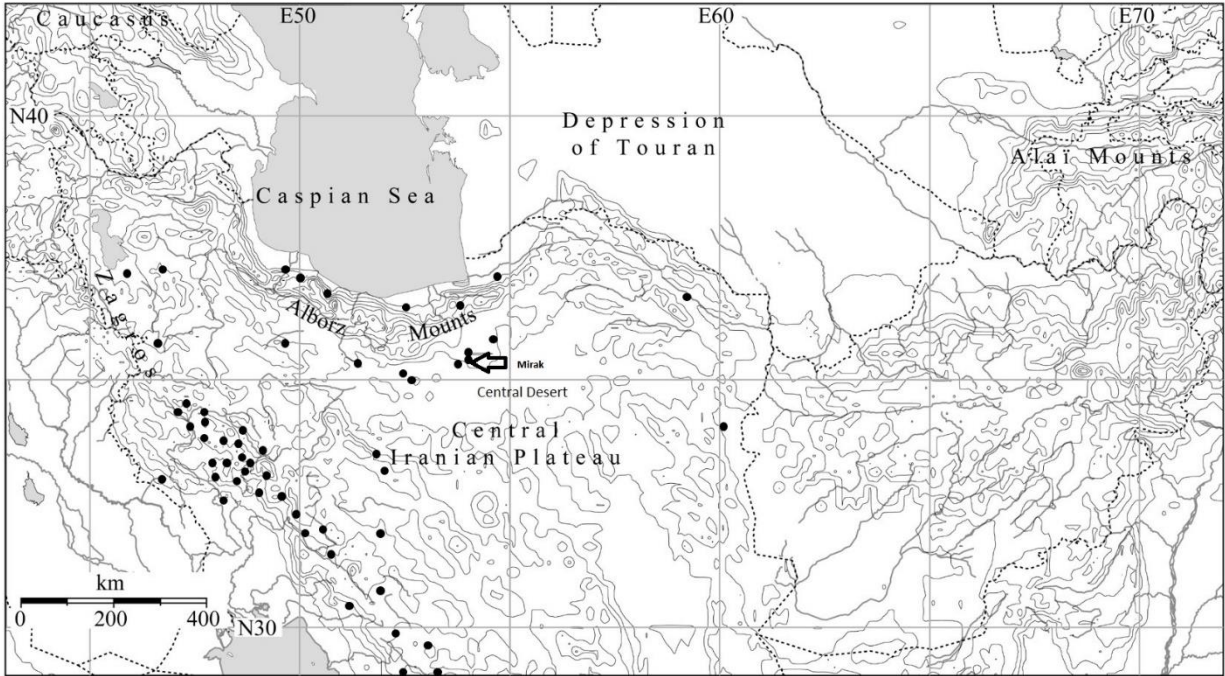
Notched/Denticulate Blade	0	5	3	8	2.2
Point on Blade	0	0	2	2	0.6
Retouched Blade	0	8	7	15	4.2
Scraper on Blade	0	2	4	6	1.7
Naturally Backed knife	0	1	1	2	0.6

<b>Other Tools</b>	<b>0</b>	<b>0</b>	<b>6</b>	<b>5</b>	<b>4</b>	<b>1.8</b>	<b>10</b>	<b>2.8</b>
<b>Sum</b>	<b>10</b>	<b>100</b>	<b>121</b>	<b>100</b>	<b>225</b>	<b>100</b>	<b>356</b>	<b>100</b>

626

627

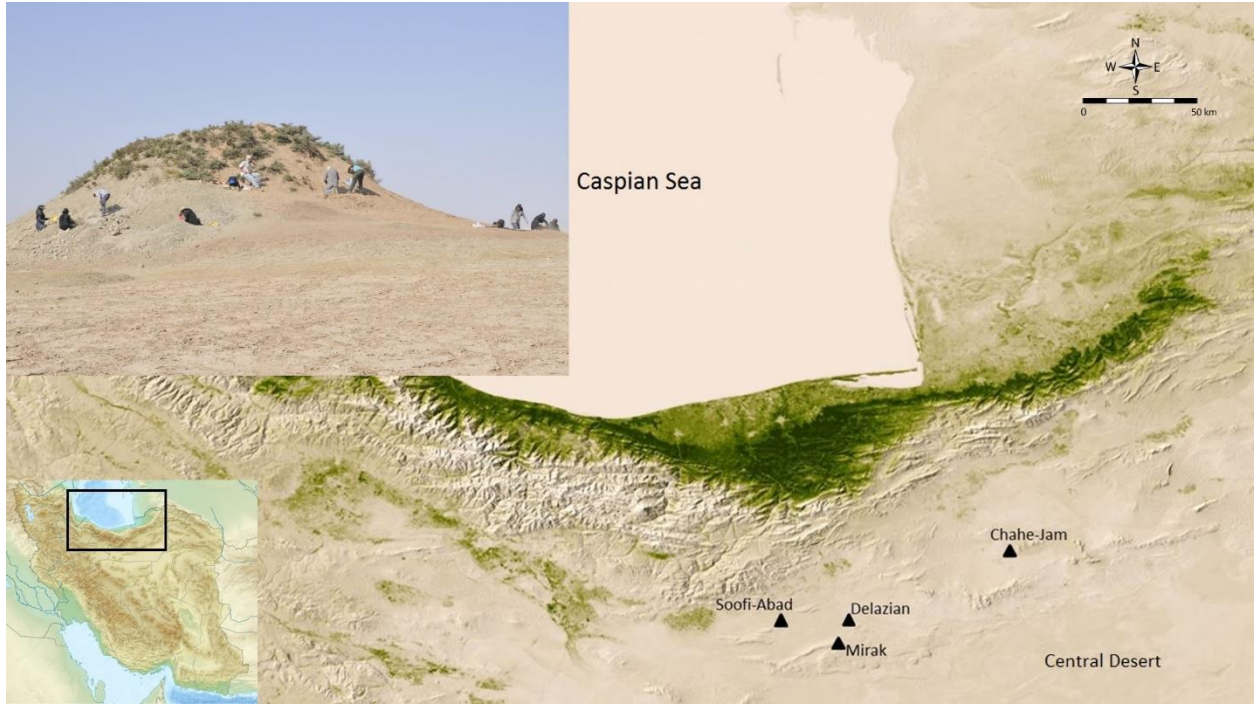
628



629

630 Fig. 1

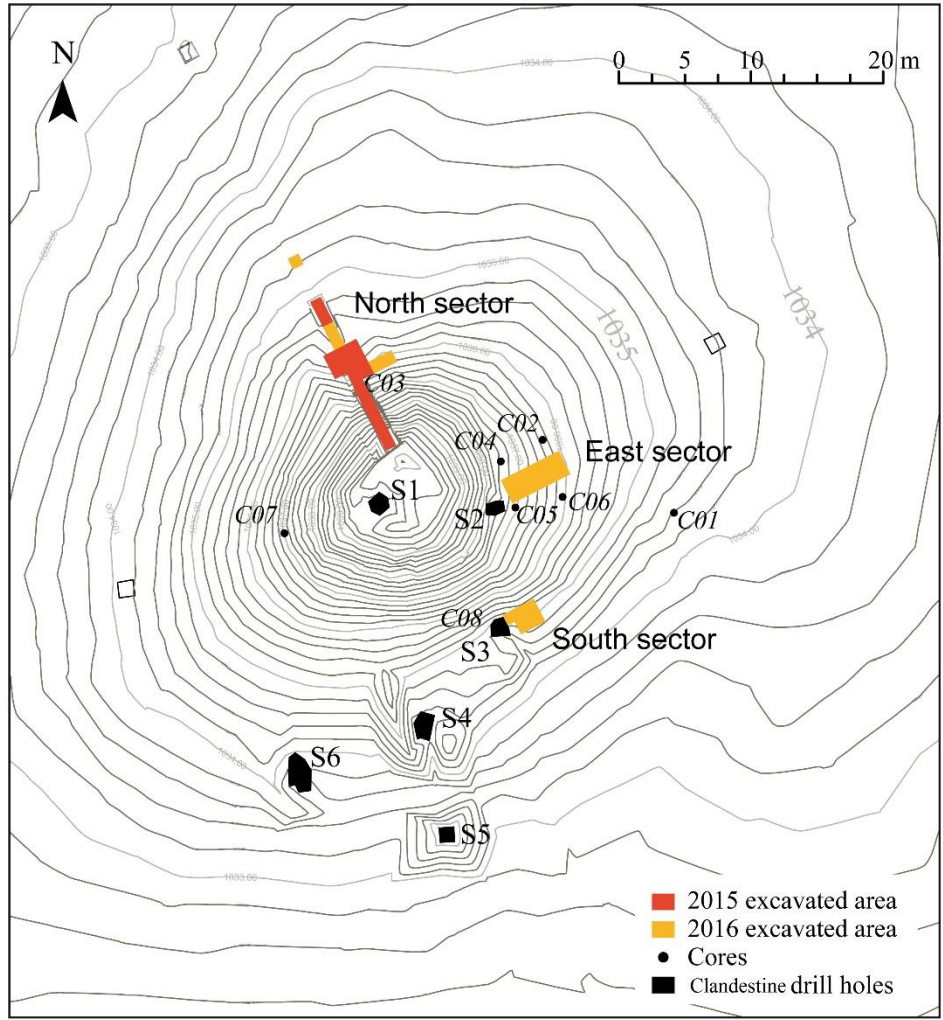
631



632

633 Fig 2

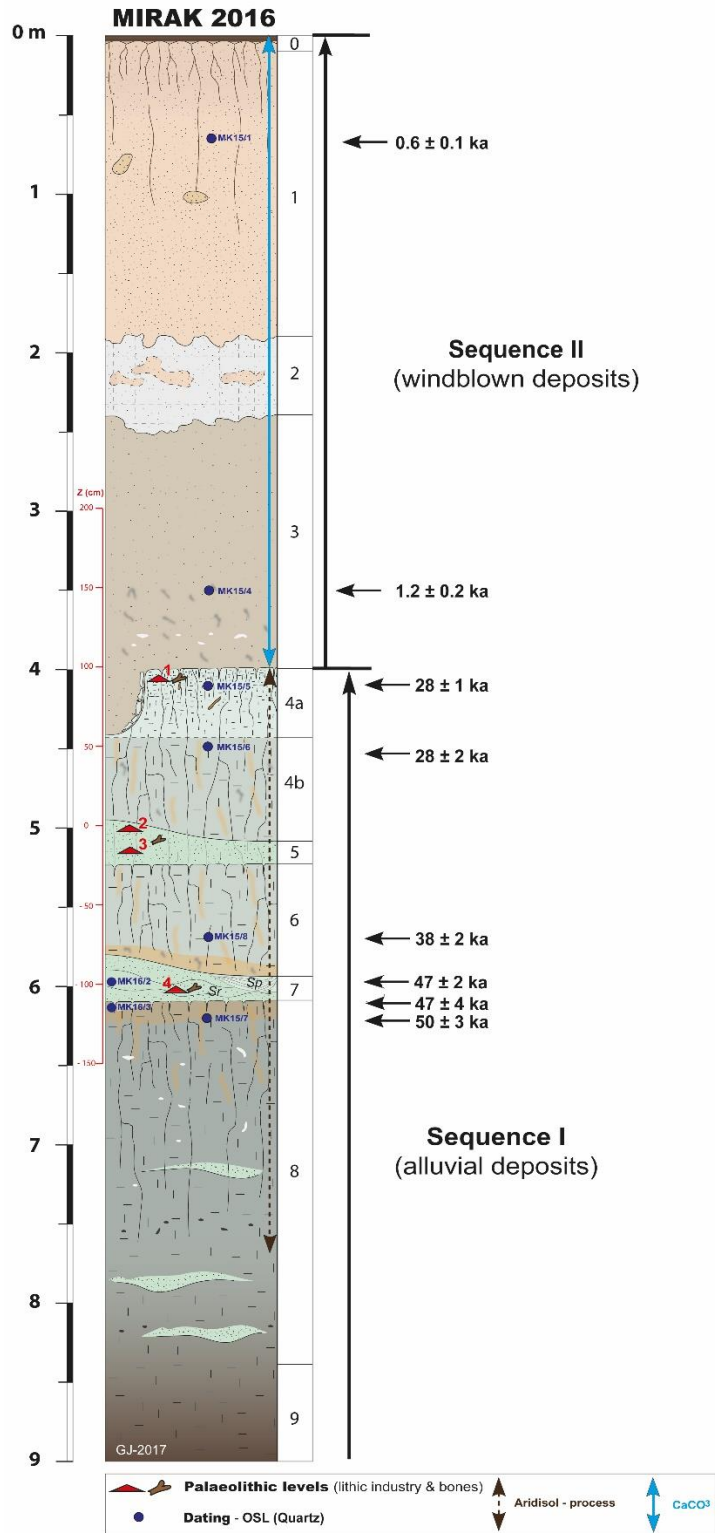
634



635

636 Fig.3

637

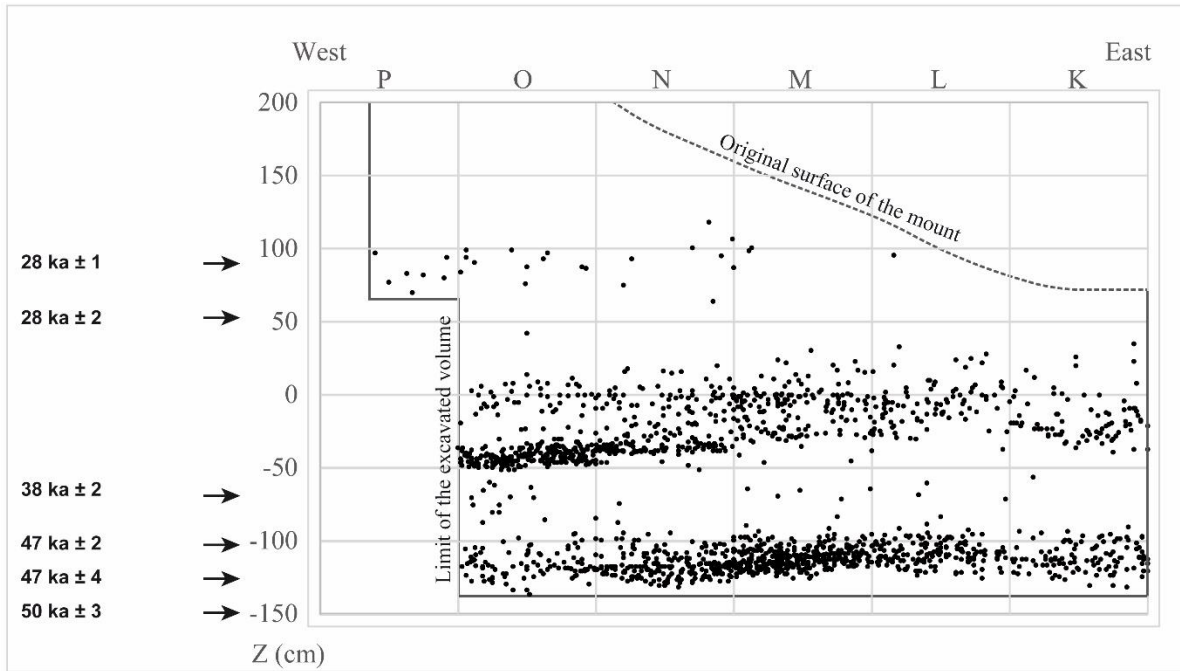


638

639 Fig.4

640





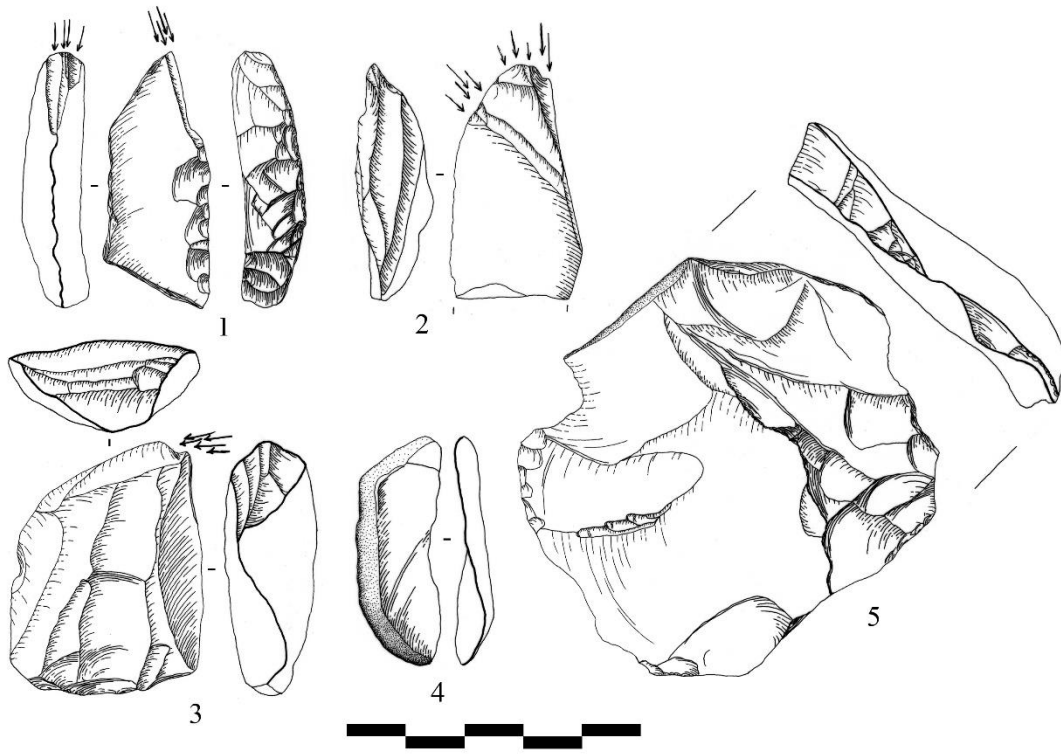
642

643 Fig.5

644

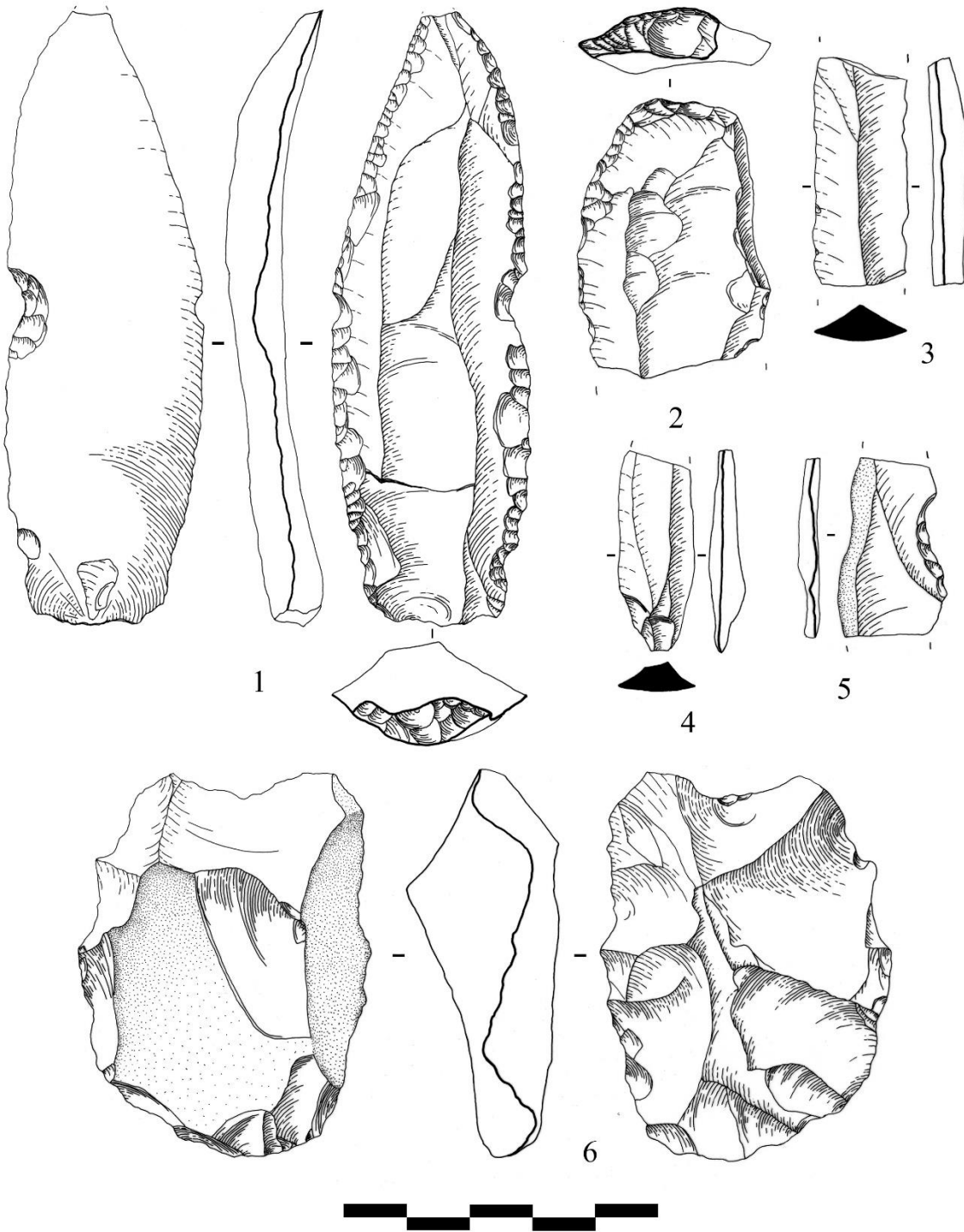
645

646



647

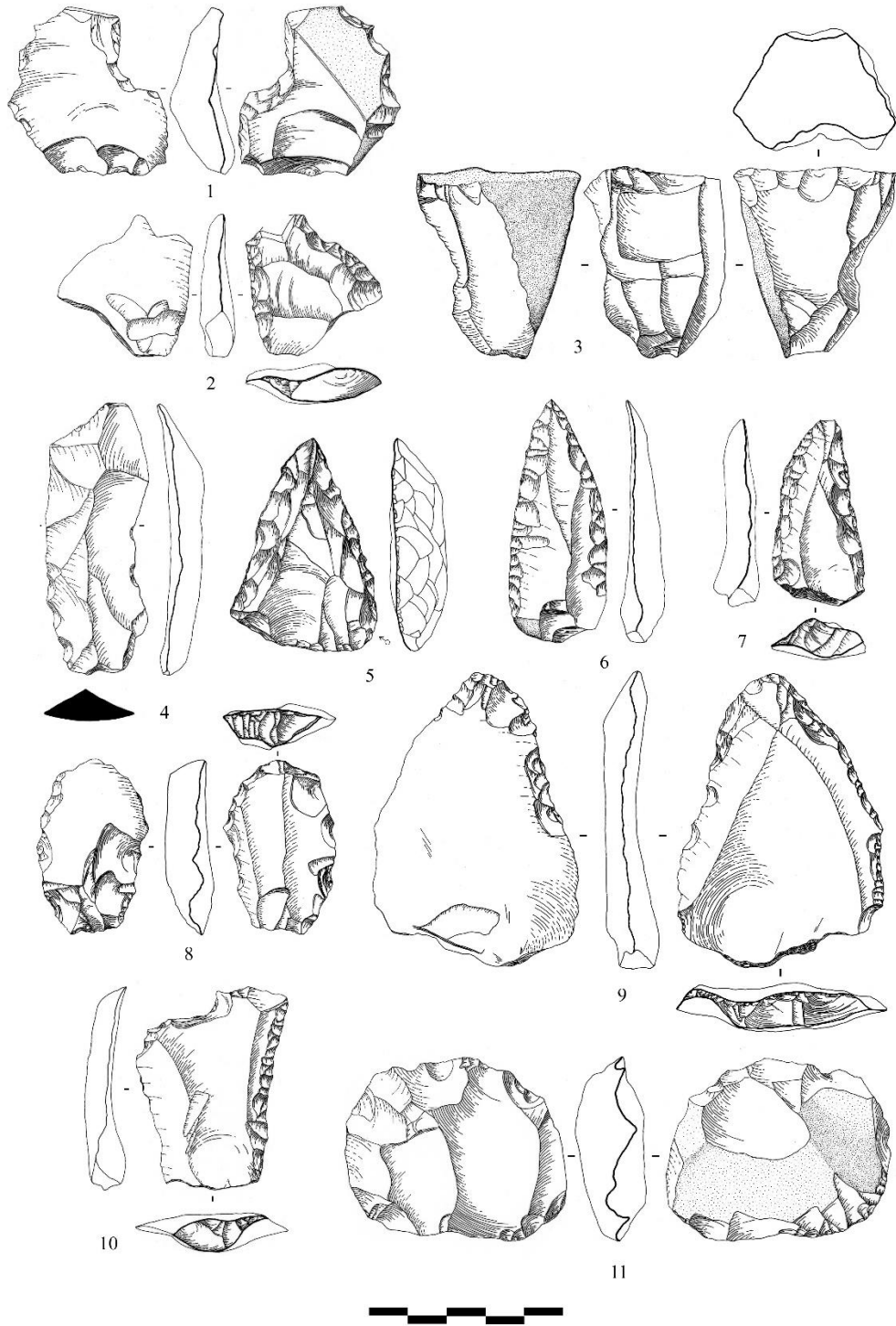
648 Fig.6



649

650 Fig.7

651



656 SUPPLEMENTARY MATERIAL

657

658 OSL – Methods and references

659 Samples for luminescence dating were prepared following standard procedures to extract 80-140  $\mu\text{m}$   
660 grains of both quartz and K-feldspar. OSL and post-IR IRSL at 290° C (pIRIR290) measurements were  
661 performed on multi-grain aliquots (several hundred grains were measured for each aliquot). Standard  
662 SAR protocols (see for quartz: Wintle and Murray 2000; for K-feldspar: Thiel et al. 2011; Buylaert et al.  
663 2012) were implemented (see e.g. the protocols used in Guérin et al. 2015). Gamma and beta dose rates  
664 were determined from high resolution gamma spectrometry; the measured concentrations in  
665 radioelements were converted in dose rates using the factors from Guérin et al. (2011), modified for the  
666 effect of water after Guérin and Mercier (2012) and for the effect of grain size attenuation after Guérin  
667 et al. (2012). Cosmic dose rates were determined after Prescott and Hutton (1994) based on the  
668 thickness of sediment overburden.

669 For two samples (MK15/6 and MK15/8), an important disequilibrium in the U-series was observed,  
670 which might be linked with the above-mentioned level fluctuations in the water table and/or the  
671 presence of iron hydroxide precipitation. Without further information about the nature (leaching of  $^{238}\text{U}$   
672 or uptake of  $^{226}\text{Ra}$ ) and timing of the disequilibrium (Guibert et al., 2009), the ages presented in this  
673 study were calculated assuming a linear uptake model, which seems to be the most parsimonious  
674 hypothesis and corresponds to a midway scenario (and set of ages). It should be noted here that  
675 humidity of the sediment was determined from measurements at sampling time; this present-day  
676 moisture content was considered to be representative of that during burial (except for sample MK16/2:  
677 the measured water content was  $5\pm 2\%$ , which seems a bit low compared to other values; arbitrarily, we  
678 used  $10\pm 5\%$ . Ongoing work should in the future allow refining the water concentrations for all sediment  
679 samples).

680 Quartz OSL and K-feldspar post-IR IRSL ages are in agreement for all samples (with a slight  
681 overestimation of K-feldspar compared to quartz, which is common since the resetting of K-feldspar  
682 post-IR IRSL signals is much slower than that of quartz OSL) but four (the two oldest samples, MK15/8  
683 and MK15/7 as well as MK16/2 and MK16/3 which are belong to eastern section ). For the four latter  
684 samples, assuming that quartz OSL was totally reset before sediment deposition, the residual doses for  
685 the K-feldspar post-IR IRSL correspond to 49 Gy ,74 Gy, 54 Gy and 282Gy for samples MK15/8 ,MK15/7,  
686 MK16/2 and MK16/3, respectively. These relatively high residual doses(especially for MK16/3), in  
687 comparison with commonly reported values of  $\sim 5\text{-}20$  Gy for well bleached samples (e.g., Buylaert et al.  
688 2012) indicate that light exposure of the sediment prior to burial was insufficient to completely reset the  
689 K-feldspar post-IR IRSL signal. This observation might be the result of the above-mentioned shallow  
690 water deposition during flood events. In any case, the K-feldspar post-IR IRSL ages should be regarded as  
691 maximum ages. Nevertheless, such a poor bleaching of the K-feldspar signal does not necessarily imply  
692 that quartz OSL was not fully bleached (Murray et al. 2012) since the reset of quartz OSL during light  
693 exposure is several orders of magnitude faster than that of K-feldspar post-IR IRSL (Buylaert et al. 2012).

694 In fact, Guérin et al. (2015) already observed such high residual doses (60-80 Gy) for K-feldspar post-IR  
695 IRSL signals from samples for which multi-grain quartz OSL was well-bleached, as indicated by the  
696 comparison with radiocarbon ages.

697

698

699 Buylaert, J.P., Thiel, C., Murray, A.S., Vandenberghe, D.A.G., Yi, S., Lu, H., 2011. IRSL and post-IR IRSL  
700 residual doses recorded in modern dust samples from the Chinese Loess Plateau. *Geochronometria* 38,  
701 432e440.

702 Guerin, G., Mercier, N., Adamiec, G., 2011. Dose rate conversion factors: update. *Anc.TL* 29, 5-8.

703 Guerin, G., Mercier, N., 2012. Preliminary insight into dose deposition processes in sedimentary -media  
704 on a grain scale: Monte Carlo modelling of the effect of water on gamma dose rates. *Radiation*  
705 *Measurements* 47, 541e547.

706 Guerin, G., Mercier, N., Nathan, R., Adamiec, G., Lefrais, Y., 2012. On the use of the infinite matrix  
707 assumption and associated concepts: a critical review. *Radiation Measurements* 47, 778-785.

708 Guerin, G., Frouin, M., Talamo, S., Aldeias, V., Bruxelles, L., Chiotti, L., Dibble, H.L., Hublin, J.J., Jain, M.,  
709 Lahaye, C. 2015. A multi-method luminescence dating of the Paleolithic sequence of La Ferrassie based  
710 on new excavations adjacent to the La Ferrassie 1 and 2 skeletons. *Journal of Archaeological Science*  
711 58,147-166.

712 Guibert,P., Lahaye, C., Bechtel, F., 2009. The importance of U-series disequilibrium of sediments in  
713 luminescence dating: A case study at the Roc de Marsal Cave (Dordogne, France). *Radiation*  
714 *Measurements* 44, 223–231.

715 Murray, A.S., Thomsen K.J., Masuda, N. Buylaert J.P. Jain M.,2012. Identifying well-bleached quartz  
716 using the different bleaching rates of quartz and feldspar luminescence signals. *Radiation*  
717 *Measurements* 1-8.

718

719

720

721